Received: August 2, 2022. Revised: October 30, 2022.

INASS

International Journal of
Intelligent Engineering & Systems

http://www.inass.org/

Performance Analysis of Indoor Light Fidelity Technology Propagation Using Fixed and Movable LED Panels

Fauza Khair[1]* **I Wayan Mustika[2]*** **Dodi Zulherman[1]** **Fakhriy Hario P[3]**

[1]*Institut Teknologi Telkom Purwokerto, Indonesia*
[2]*Universitas Gadjah Mada, Indonesia*
[3]*Universitas Brawijaya, Indonesia*
* Corresponding author's Email: wmustika@ugm.ac.id

Abstract: Light fidelity (Li-Fi) offers communication services with a wide bandwidth and is one of the options for telecommunications services in the future, especially indoor communication. However, Li-Fi requires accurate device positioning for line of sight (LOS) conditions to meet the main requirement for light communication. Conventional Li-Fi design models require a more dynamic transmitter and receiver device settings but can still serve LOS communication well. This study aims to design a Li-Fi communication model by varying the transmitting devices, such as the use of fixed and movable LEDs, and receiving devices, such as the addition of optical rectangle filters, low-pass filters, and trans-impedance amplifiers. The focus of observation includes the effect of changes in wavelength, data transmission speed, transmitter half-angle, irradiance angle, and incidence angle, as well as field of view (FOV) on received power parameters, signal-to-noise ratio, Q-factor, and bit error rate (BER). On the basis of the test results, the performance of all wavelength variations meets the ITU-T standard up to a variation of the transmission distance of 8 m, where the use of fixed and movable LEDs does not result in a significant difference in performance. The test results indicate that the wavelength parameter affects the signal quality due to the spectral response and LEDs emission. For short distances, the wavelength of 450 nm has better performance, whereas for distances up to 8 m, the wavelength of 650 nm has a better performance than other variations. Furthermore, increasing the transmitter half-angle increased the BER value and drastically decreased the Q factor. The use of a smaller FOV is recommended, as shown from the increase in distance resulting in a significant decrease in performance. The proposed system model can also be used for bit rates up to 30 Mbps, although it is only reliable up to 6 m. As for the 40 Mbps variation, the 75° half-angle transmitter, 60° FOV, and 90° FOV variations do not meet the standard. The two system models do not have a significant difference in performance. Thus, using movable LED instead of fixed LED will make the system more dynamic with a well-maintained LOS.

Keywords: Indoor Li-Fi, Fixed LP, Movable LP, Bit rate, FOV, Transmitter half-angle.

1. Introduction

The use of a limited frequency spectrum in radio wave-based wireless communication in the last decade has made it difficult to keep up with wireless communication technology development. Aside from the capacity being unable to match customer demand, the growth of wireless service users also demands more spectrum efficiency. The optical-based wireless communication system is an option to resolve the problems in radio communication. Optical wireless communication offers high data transmission rates with greater bandwidth than radio. One example of the use of wireless optical technology is light fidelity (Li-Fi) [1, 2].

Li-Fi, also known as optical wireless communications, uses light as a medium to transmit information, which refers to as visible light communication (VLC) [3]. VLC is a data communication medium that uses visible light with a frequency between 400 THz (780 nm) and 800 THz (375 nm) as an optical carrier data transmission using rapid light pulses to transmit

information signals wirelessly [4]. Li-Fi follows the VLC standard, namely the IEEE 802.15.7 standard which has three types of physical layer (PHY) where the operating range of PHY I is from 11.67 kb/s up to 266.6 kb/s, PHY II is from 1.25 Mb/s up to 96 Mb/s, and the PHY III is 12 Mb/s up to 96 Mb/s [5], respectively.

Several studies have shown that Li-Fi supports communication technology in smart cities; enables the Internet of Things and the Internet of Everything; and supports super-fast wireless internet, aircraft, health technologies, underwater work, traffic control, disaster management, education, and defense [6-11]. Moreover, Li-Fi technology, especially for indoor use, has emerged as a new alternative that is more environmentally friendly, healthier, and cheaper than Wi-Fi technology [3]. Li-Fi technology operates using a lamp driver consisting of an LED and a lamp bulb, and it works with the binary principle of 0 and 1. Data are sent by dimming or blinking at the speed of nanoseconds, making it difficult for the eye to see. Furthermore, Li-Fi technology uses an LED panel system categorized into fixed LP and movable LP, which provides network connectivity coverage and meets different line of sight (LOS) conditions for each emitted LED panel [1]. In addition, a model and design of Li-Fi technology that utilizes the amplifier and filtering at the receiver side have shown an increased quality of the received signal [12].

Information transmission parameters such as source and channel coding techniques and the direction of transmission affect the spectrum of the received signal [1, 2, 12-14]. Furthermore, the reception angle, the reception area (field of view [FOV]), and the detector area are the parameters that determine signal processing in the photodetector [2, 13, 15]. Therefore, several considerations exist to obtain a signal quality that meets telecommunication standards. Some are information delivery from the source, transmitting the LED source on the transmitter side, signal propagation through the wireless medium, and receiving parameters on the receiving side. Therefore, this research comprehensively proposes a Li-Fi technology system model using fixed and movable LED panels by placing an optical rectangle filter on the photodetector and placing a transimpedance amplifier (TIA) and a low-pass filter on the receiver side as system development for conventional indoor Li-Fi [12].

This study analyzes the transmission signal quality based on the parameters of the transmission system block and signal propagation, including variations in bit rate, transmitter half-angle, irradiance angle, and acceptance angle. Furthermore, the received signal quality will be analyzed based on the received power value parameters, signal-to-noise ratio (SNR), and bit error rate (BER). Moreover, this study will vary the value of the receiver's reception angle or FOV to know the overall signal quality characteristics.

2. Related work

Several transmitting and receiving quality parameters such as angle of irradiance, angle of incidence, and SNR have been simulated for indoor Li-Fi utilization using RGB LEDs. This experiment uses three scenarios: fixed, movable, and hybrid LED panels. The scenarios vary the data modulation scheme in the form of on-off keying (OOK), pulse position modulation (PPM), variable PPM, overlapping PPM, and optical spatial modulation. The simulation shows an increased value of the angle of irradiance from 65° to 78°, where the angle of incidence remains at 45°, resulting in a decreased SNR value [1].

The light configuration in the room using a VLC system also plays an important role in the propagation of the light signal. Mathematical and theoretical models of VLC communication have identified several factors in determining signal propagation: room size, distance, receiver plane, half-power angle, center luminous intensity, reflectance factor of the walls, optical filter gain, photodiode responsibility, optical concentrator refractive index, and constant noise-related and a detector area in the photodetector [2]. Numerical calculations show that an increase in the FOV value causes the acceptability and SNR value to decrease. Meanwhile, increasing the FOV value increases the optical concentrator's gain value so that the photodetector's sensitivity decreases. In addition, the maximum distance between the two LEDs will affect the switching process. Whereas the hysteresis margin H increases, the overlapping distance must also be increased. However, this numerical method VLC model did not consider bit rate parameters and variations of test parameters such as transmitter half-angle, irradiance, and incidence angle. The Li-Fi-based indoor communication system's main potential and the challenges Li-Fi network faces include the modulation process, transmission direction, and propagation conditions. Hence, Wi-Fi and Li-Fi networks need to be integrated; this is related to the modulation process, such as the OOK type of the LED source panel, and is limited to LOS conditions. The utilization of Li-Fi is still limited in this LOS condition; the alignment of the FOV is

necessary to maximize channel response. Shadowing effects also affect LOS propagation, where interference from light sources, such as the sun and other electric light, can affect Li-Fi communication. The Li-Fi system makes each LED bulb a wireless hotspot [3].

The choice for VLC network architecture, LED panel frequency spectrum, and modulation such as OOK, VPPM, and M-CSK have become important topics for discussions [4]. OOK modulation has a higher data rate than VPPM, with an optical clock of up to 120 MHz. The basic architecture of the VLC network consists of optical filters/drivers on the transmitter side, while electrical filters and amplifiers are on the receiving side. The LED color used relates to determining the available VLC frequency spectrum from 380 nm to 750 nm [4].

The development of Li-Fi system design has been conducted with regard to the design and functionality of indoor Li-Fi to provide a better wireless communication model [12]. To achieve the best results and accuracy, this study examined and tested an entire system at different values with various parameters. These parameters are various transmitting angles, data rates, distances, frequencies, the responsiveness of PIN diodes, different filters, detector areas, transmitted pulses, and modulation schemes. Using LP Chebysev filter on the receiving side produces a minimum BER value of 10^{-47}[12]. Additionally, the increase in data rate and the angle of the transmitter have significant effects on increasing the value of BER. However, this study does not consider variations in the wavelength of the LED transmitter, bandwidth, receive power, SNR, and variations in transmit and receive angles.

The performance evaluation of a Li-Fi network with multibeam LEDs on moving user equipment considers some parameters. The parameters are half-intensity angle LED, FOV, optical filter gain, effective photodetector area, and refractive index [13]. Theoretical calculations and simulation results show that the best-received signal quality is with a beam angle of 30°, which is limited to LOS conditions. Analysis and simulation of the Li-Fi network quality for various distances and considering the angle of incidence, LED power, photodiode responsiveness, and transmission coefficient of the optical filter resulted in a drastic decrease in SNR to at least 90 dB. Increasing the distance from 2 m to 6 m lowers the SNR value to 50 dB and decreases to 25 dB with the transmitter and receiver distance of 12 m. However, this study does not consider the bit rate and the transmitting and receiving angle of transmitter and receiver (FOV) [16]. The room's LED transmitter and photodetector placement are related to the epsilon LED model and OOK modulation [17]. Utilization of digital input with PSK modulation and optical OFDM system from four LED panels with a photodetector in a $6 \times 6 \times 3.5$ m room proves that position and distance significantly affect the quality of the received signal. The system model is not directly network-dependent and available to use after LED configuration and calibration.

The cell concept applies to communications where an increase in cell size increases the distance and requires adjustment to the transmitter height [18]. Increasing the distance or height of the transmitter and the incidence angle value resulted in an expansion of the light beam, which is proportional to the size of the circular area. The performance of the handover algorithms in Li-Fi networks, including closest access point (CAP) and maximum channel gain (MCG) handover algorithms, shows the effect of LED half-intensity angle and receiver FOV [15]. This effect proves that the MCG handover decision performs better than the CAP handover decision with SIR, and the highest gain is obtained at a beta value of 45°.

Theoretically, a wide FOV can capture a larger view regarding the reception parameters. If the receiver can distinguish visible light from the transmitter in FOV, then all data from the transmitter can be received. However, a receiver with a wide FOV is prone to more ambient light noise than a receiver with a narrow FOV, which means an increase in FOV implies a decrease in the value of SNR and an increase in the value of BER [19]. In addition, the increase in bit rate increases the BER value, where the average SNR value decreases according to the increase in the number of LED colors (wavelengths) used. The decrease in the average SNR is due to mismatch and synchronization when the receiver is tilted 45° [20]. The use of the LED working frequency of 650 nm was implemented successfully by considering the combination of FOV and Hadamard coded modulation [21]. This implementation proves that PAPR from HCM is smaller than OFDM.

3. Proposed indoor Li-Fi system model and parameter

The proposed system design in this study uses the concept of an indoor optical wireless link consisting of a data source system block and an electrical-to-optical conversion mechanism on the transmitter side. The receiving system block consists

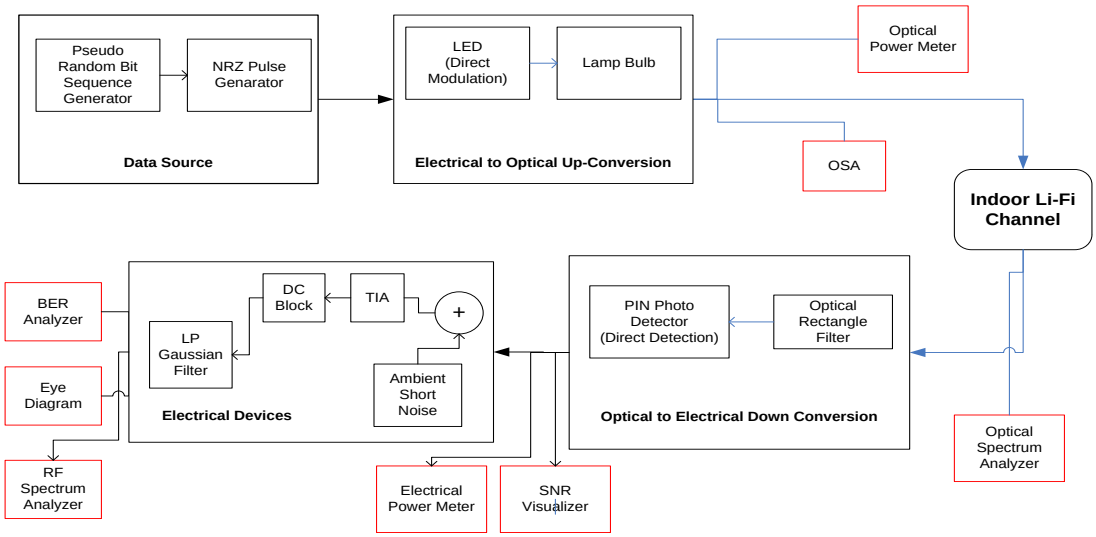

Figure. 1 Proposed scheme of indoor Li-Fi using fixed and movable LED panels

of an optical-to-electrical down conversion system and an electrical device, as shown in Fig. 1.

The system block circuit in Figure 1 has several components that work together for the Li-Fi system to work optimally. The transmitter components that need attention are the PRBS generator and non-return to zero (NRZ) pulse generator components as digital data inputs and LEDs as optical sources that work using the principle of direct optical modulation. PRBS provides information bit in the form of an electrical signal. The bit sequence is designed to correspond with the characteristics of random data, which is formulated as follows:

$$N = T_w B_r \tag{1}$$

$$N_G = N - n_l - n_t \tag{2}$$

where, T_w is the global time window parameter, and B_r is the bit rate parameter. The bit number results are N_g. n_l and n_t are the number of leading zeros and the number of trailing zeros, respectively. The bit sequence is then forwarded to the NRZ pulse generator block as channel encoding, which produces rectangular NRZ electrical pulses in the following exponential mode.

$$E(t) = \begin{cases} 1 - e^{-\left(t/C_r\right)} & ,0 \le t \le t_1 \\ 1 & ,t_1 \le t \le t_2 \\ e^{-\left(t/C_f\right)} & ,t_2 \le t \le T \end{cases} \tag{3}$$

where C_r is the rise time coefficient, C_f is the fall time coefficient, and T is the bit period. Time point t_1 and t_2, along with C_r and C_f, are numerically set to generate pulses in sync with the rise and fall time parameter values. The LED converts the binary bits that pass through the NRZ encoding, using a direct-modulation scheme, into analog data modulated into visible light. The emitted LEDs operate at a frequency of 450 nm to 750 nm with a bandwidth of 0.03 nm. The current conversion to optical power is related to the LED responsiveness or slope efficiency. The formula to calculate the LED responsiveness is as follows:

$$P = \eta . h . f \frac{i(t)}{q} \tag{4}$$

where η is the quantum efficiency, h is the Planck's constant, f is the frequency, q is the electron charge value, and $i(t)$ is the modulation current signal. The modulation characteristic depends on the electron lifetime and the diode device. The characteristic modeled by the transfer function applied to the current is as follows:

$$H(f) = \frac{1}{1 + j2\pi f(\tau_n + \tau_{rc})} \tag{5}$$

where τ_n is the electron lifetime, and τ_{rc} is the RC constant. Table 1 shows the test parameters on the transmitter section.

The light emitted from an LED surrounded by a lamp bulb is assumed to be Lambertian radiation because it obeys the Lambertian cosine law. Lambertian radian intensity is the emitted or reflected flux, and then it is received by a solid

Table 1. Transmitter specification

Parameter	Value	Unit
Bit rate	20, 30, 40	Mbps
LED frequency	450–650	nm
Bandwidth	0.03	nm

angle per unit, where the flux emitted is per unit area [15]. Therefore, the Lambertian flux intensity is written as [2, 12]

$$R_0 = \left(\frac{m+1}{2\pi}\right) cos^m \theta \quad (6)$$

$$m = -\left(\frac{ln2}{ln\left(cos\theta_{1/2}\right)}\right) \quad (7)$$

where θ is the radiation angle, and m is the Lambertian order obtained from Eq. (7), where the variable $\theta_{1/2}$ is the value of semi-angle transmitter at half power. For example, suppose an LED's lamp driver emission pattern emits symmetrical radiation. In that case, the amount of radiation is the LED's emitting power multiplied by the Lambertian flux's intensity. Then, a photodetector will receive the emitted radiation at a certain receiving angle. The value of power amount per area received *W/cm²* refers to Eq. (6). Therefore, Eq. (8) is written as

$$I_s[d, \theta] = \frac{P_t \times R_0(\theta)}{d^2} \quad (8)$$

where d is the distance between the LED and the receiver. The received power can be calculated using Eq. (9)

$$P = I_s[d, \theta] \times A_{eff}(\psi) \quad (9)$$

Where A_{eff} is associated with a receiver structure consist of a filter, a lens having a gain, and a detector area that can be calculated by

$$A_{eff}(\psi) = \begin{cases} A_{det} T_s(\psi) g(\psi) cos(\psi) & 0 \le \psi \le \psi_c \\ 0 & \psi > \psi_c \end{cases} \quad (10)$$

where A_{det} is the detector area, T_s is the filter transmission gain, g is the lens gain, ψ_c is the FOV receiver, and ψ is the angle of incidence to the receiving axis. Lens gain is calculated with Eq. (11), where n is the concentrator refractive index.

$$g(\psi) = \begin{cases} \frac{n^2}{sin^2 \psi_c} & 0 \le \psi \le \psi_c \\ 0 & otherwise \end{cases} \quad (11)$$

$$H(0)_{LOS} = \begin{cases} \frac{(m+1)A}{2\pi d^2} cos^m(\theta) T_s(\psi) g(\psi) cos(\psi) & 0 \le \psi \le \psi_c \\ 0 & \psi > \psi_c \end{cases} \quad (12)$$

The DC channel gain in the first reflection formulated in Eq. (12) has the same considerations. Through substitution in Eq. (9), the received power value is known and formulated in Eq. (13).

$$P_r = \begin{cases} \frac{(m+1)A_{det}}{2\pi d^2 sin^2 \psi_c} cos^m(\theta) T_s(\psi) n^2 cos(\psi) & 0 \le \psi \le \psi_c \\ 0 & \psi > \psi_c \end{cases} \quad (13)$$

The optical signal spectrum received by the photodetector is the filtering result obtained by an optical rectangle filter to anticipate pulse widening due to the transmission angle, LED source linewidth expansion, and the difference in the reception area of the light sensor due to the increasing FOV. The formula for the filter transfer function is

$$H(f) = \begin{cases} \alpha, \left(f_c - {}^{B}/_{2} < f\right) < f_c + {}^{B}/_{2} \\ d \end{cases} \quad (14)$$

with α is the insertion loss parameter, d is the depth parameter, f_c is the filter center frequency, B is the bandwidth parameter, and f is the frequency.

This study will compare the performance of Li-Fi communication propagation using fixed and movable LP. The basic difference between the two scenarios is the emission direction, where the value for the irradiance angle of fixed LP is 0°. The value for the irradiance angle of movable LP is 20°. This study will conduct tests with various distance parameters between the source LED and the photodetector, transmitter half-angle, and FOV concentrator, as shown in Table 2.

The signal will be received and converted into an electrical signal again by a PIN photodetector using a direct detection scheme. The optical signal becomes an electric current based on the device's responsiveness, which is affected by noise in the form of dark current, thermal noise, and shot noise. The researchers downsampled the input optical signal and optical noise, converted them into an electrical signal, and separated them from noise according to the responsiveness of the PIN. The researchers added short thermal noise and thermal

Table 2. Propagation parameter.

Parameter	**Fixed LP**	**Movable LP**
Distance	3 m up to 8 m	3 m up to 8 m
Detector Area	1.5 cm^2	1.5 cm^2
FOV *Concentrator*	30° up to 90°	30° up to 90°
Index Concentrator	1.5	1.5
Tx Half-Angle	30° up to 75°	30° up to 75°
Irradiance Angle	0°	20°
Incidence Angle	20°	20°

noise as electrical noise signals, and using Eq. (15) and can thus calculate the sample size of the optical input signal data in the time domain, and with the short variance in Eq. (16), and thermal noise values in Eq. (17).

$$i(t) = rP(t) + i_d \tag{15}$$

$$\sigma^2_{short-S} = 2B_{e.}(rP_s + i_d) \tag{16}$$

$$\sigma^2_{thermal} = \frac{4k_BT}{R_L} ENB \tag{17}$$

where B_e is the equivalent noise bandwidth from PIN, r is the PIN responsivity value, P_s is the signal power, i_d is the device dark current value, T is the device absolute temperature, R_L is the receiver load resistance, k_B is the Boltzmann constant, and ENB is the receiver equivalent electrical noise bandwidth. This study's test used a response of 0.2 A/W with a dark current of 10 nA.

The device's loss is analogous to the addition of noise effects with an average output power of −120 dBm or a power spectral density of −60 dBm/Hz. Then, it is amplified by a TIA with a resistor value of R of 1000 ohms. The basis of the TIA model used is a shunt feedback configuration that converts input current I_{in} into an output voltage, which can be calculated based on the following equation:

$$V_{out} = I_{in}R\frac{A}{1+A} \tag{18}$$

where A is the amplifier open-loop voltage gain. To reduce the effects of noise and nonlinearity from the given gain, filtering is performed by a low-pass Gaussian filter with the following transfer function:

$$H(f) = \alpha e^{ln\sqrt{2}\left(\frac{f}{f_c}\right)^{2N}} \tag{19}$$

where $H(f)$ is the filter transfer function, α is the insertion loss parameter, f_c is the filter cutoff frequency, N is the order parameter, and f is the frequency value.

4. Result and discussion

The basis for performance analysis of the indoor Li-Fi system using fixed and movable LP is variations in LED wavelength, transmitter half-angle, FOV, and bit rate. The results are presented in the form of optical and electrical signal spectrum characteristics after modulation and filtering, receiving power, SNR, BER, and Q factor.

4.1 LED wavelength variation

The researchers observed the effects of LED light wavelength using three values, namely, 450, 550, and 650 nm. The other transmission parameters were not varied and used the same values for all wavelength variations: transmission speed of 20 Mbps, half-angle transmission of 45°, and FOV of 45°.

On the basis of the test results, the optical signal characteristics show the peak signal amplitude value and the shift in the average power value for the 0.3 nm bandwidth range from the center frequency value. For example, Fig. 2 shows that the linewidth of the 450 nm spectrum is wider than that of the 550 and 650 nm spectrum. However, the peak amplitude of the 650 nm spectrum is slightly higher than other wavelength variations. As a result, the average signal power decreases when moving away from the center frequency, as shown in Fig 4. The 550 nm spectrum results show a wider sideband signal, as illustrated in Fig. 3, where the power drop is not too drastic compared with the 650 nm spectrum.

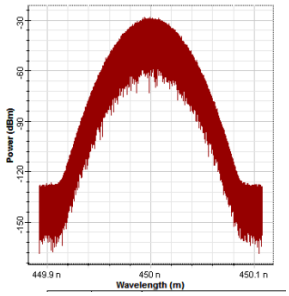

Figure. 2 Optical spectrum after DM for 450 nm

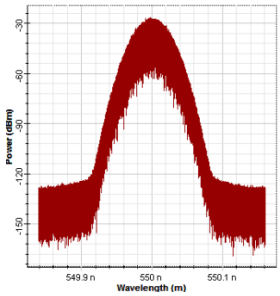

Figure. 3 Optical spectrum after DM for 550 nm

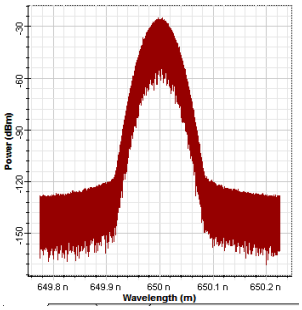

Figure. 4 Optical spectrum after DM for 650 nm

The results differ in the signal spectrum because of not only the direct modulation process but also the intensity and spectral response characteristics and the emission of each wavelength. The difference is shown in the LED material and operating frequency. For example, the light emitted at a wavelength of 450 nm has a very high intensity—up to 3500 counts—compared with the 650 nm wave with an intensity of 3000 counts. The light intensity at a wavelength of 550 nm is very low, being less than 1000 counts [4]. The utilization of the low-pass Gaussian filter on electrical devices successfully performed frequency filtering and signal power compression, as shown in Fig. 7. However, the spectrum of the noise signal generated by the short noise, as shown in Fig. 5, was not fully compressed by the TIA block and DC block, as shown in Fig. 6.

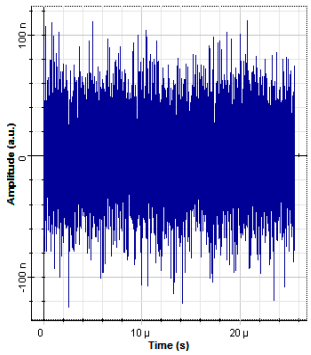

Figure. 5 Ambient short noise spectrum

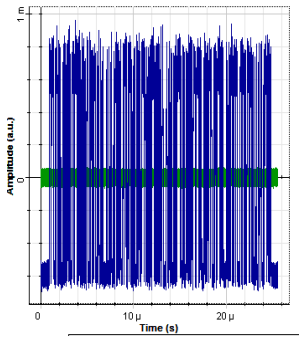

Figure. 6 Electrical received spectrum after TIA and DC block, before filtering,

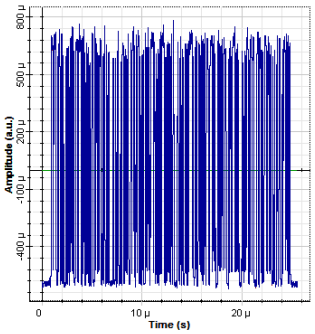

Figure. 7 Electrical received spectrum after filtering of 3 m distance

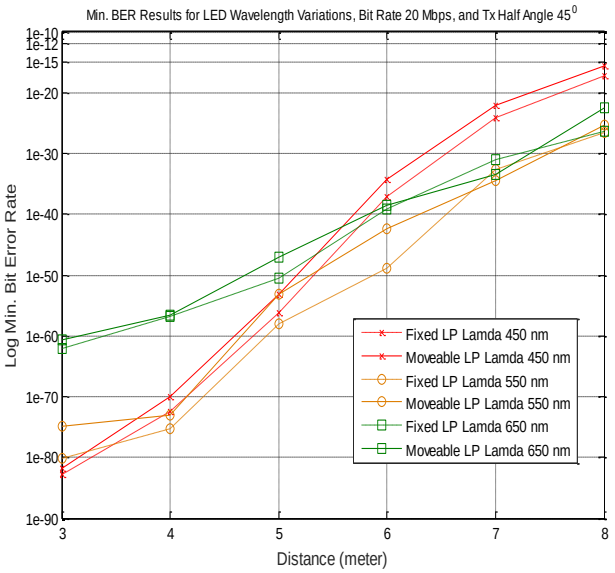

Figure. 8 Min BER result for LED wavelength variations

We then observed the effect of changes in wavelength variations on system performance through the system's ability to provide performance in line with ITU-T standards when we increased the transmission distance. The increase in transmission distance affects the reception power and reception intensity, which results in decreased signal quality, increased BER value, and decreased Q factor, as shown by the eye diagrams in Figure 8 and 9. The observations use a distance of 3 m to 8 m and compare the system performance between the smallest and largest distance.

On the basis of Figures 8 and 9, the difference in BER and Q factor values for fixed and movable LP schemes is very small for all wavelength variations. Distance is a parameter that significantly affects signal quality. At a distance of 3 m, the 450 nm frequency spectrum has the smallest BER value and the largest Q factor among all variations. The minimum BER value reaches 1.36311×10^{-83} or a Q factor of 19.3332 for the fixed scenario, and a BER value of 1.37×10^{-82} or a Q factor of 19.2137 for the movable LP scenario. The obtained values are better than those obtained in previous studies [12]. Unlike the case with the 650 nm spectrum, the BER value results of this spectrum are higher than that of 450 nm and 550 nm where the minimum value reaches 1.01×10^{-62} or equivalent to a Q factor of 16.6692 for a fixed scenario and a BER of 2.14×10^{-62} or a Q factor of 16.4866 for a movable scenario. These results have shown a significant improvement in performance compared to BER value in the previous studies [12].

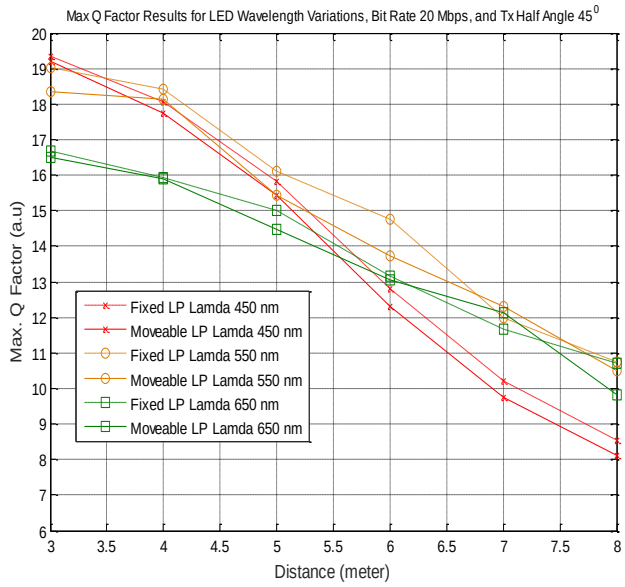

Figure. 9 Max Q-factor result for LED wavelength variations

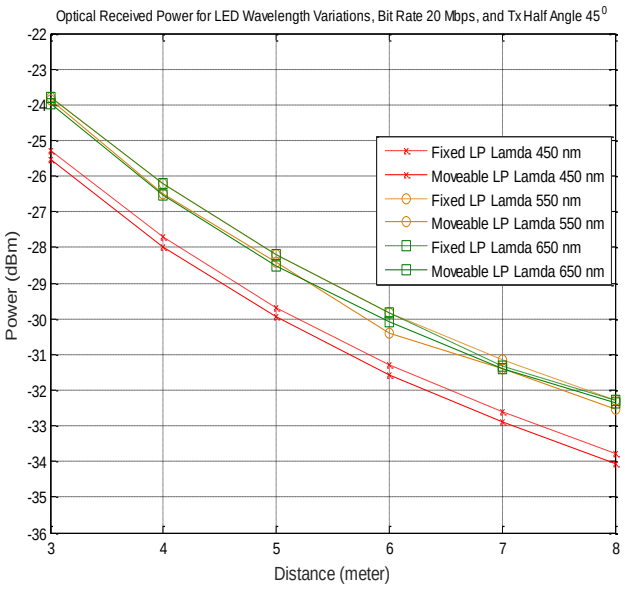

Figure. 10 ORP for LED wavelength variations

However, the increase in the BER value and the decrease in the Q factor are even more drastic in the 450 nm spectrum when the distance increases from 4 m to 8 m, although it is still below the threshold for the BER value of 10^{-12}. A moderate increase in the BER values is experienced at frequencies of 550 and 650 nm, as shown in Fig. 8 and 9, where the average BER and Q factor values are similar for the two variations. Fig. 10 and 11 show the analysis of the SNR value and optical received power (ORP) for the three scenarios. The frequency spectrum of 550 and 650 nm has almost the same high received power and SNR values for all distance variations. The decrease in the received power value for the

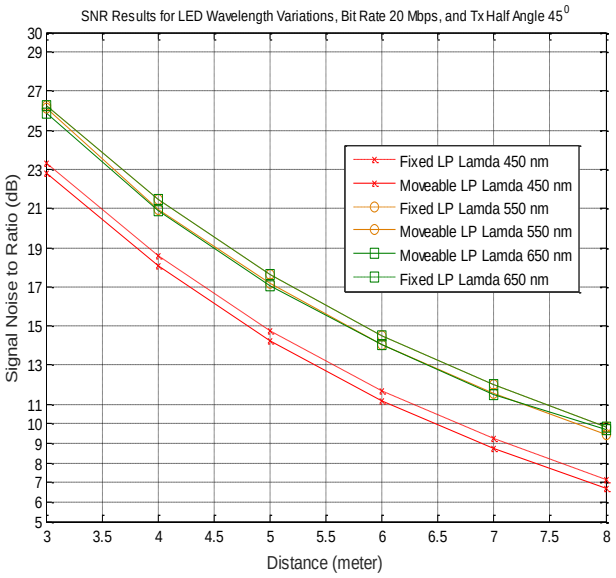

Figure. 11 SNR for LED wavelength variations

three scenarios is exactly the same. The average decrease in SNR is 3 dB to 4 dB per meter, and the decrease in the optical received power (ORP) is 2 dBm to 3 dBm per meter.

4.2 Transmitter half-angle variation

The test varies the value of the half-angle transmitter using a bit rate of 20 Mbps with a FOV value of 450. According to Eqs. (6) and (7), an increase in the value of Tx half-angle affects the Lambertian order parameters and flux intensity. The value of m = 1 is at the transmitter half-angle value of 60°, and a great value corresponds to a small angle value. Variations in the value of the tested half-angle transmitter were 30°, 45°, 60°, and 75°. Fig. 12 and 13 show that an increase in the value of the half-angle transmitter results in a drastic increase in BER and a decrease in the Q factor.

In general, the quality of the received signal due to variations in the Tx half-angle shows good performance and is not significantly different between the fixed LP and movable LED panels. Compared with other variations, the use of the 30° value has a much higher BER value and a larger Q factor, which reaches a minimum BER of 2.13×10^{-88} and a Q factor of 19.6266 for the fixed scheme and a minimum BER of 4.45×10^{-86} and a Q factor of 19.8956 for the movable LP scheme. Using a value of 75° results in the BER value approaching the threshold limit of 10^{-12}.

As a result of this variation, the results of power and SNR values received on the photodetector side are not significantly different for the fixed and movable LP schemes. Suppose the researchers

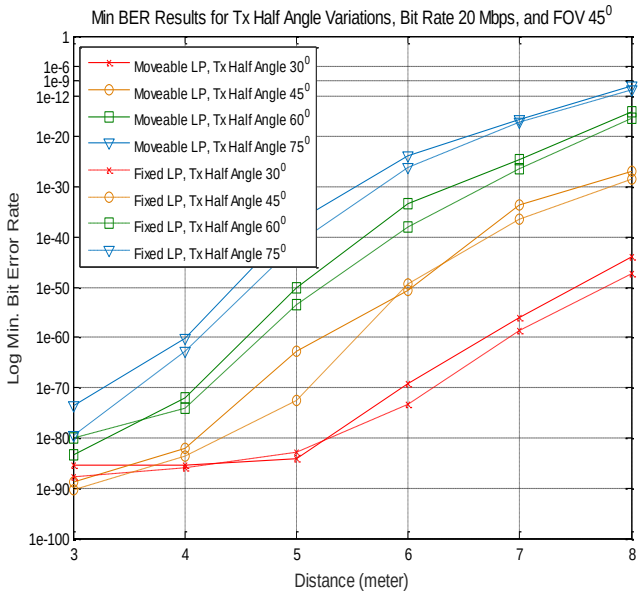

Figure. 12 Min BER for Tx half-angle variations

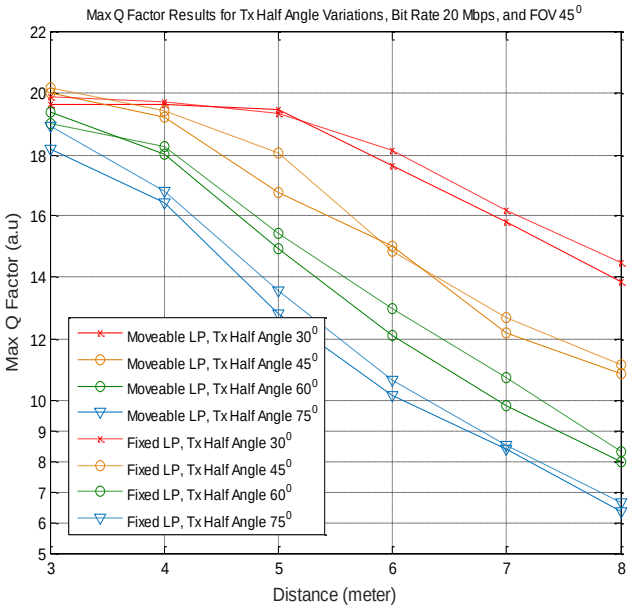

Figure. 13 Max Q-factor for Tx half-angle variations

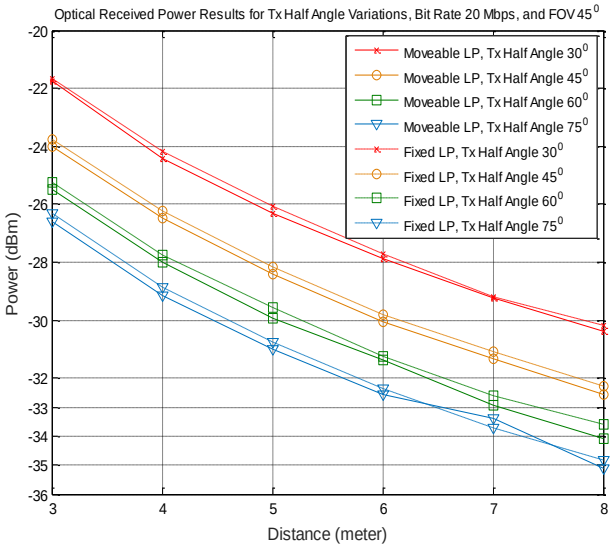

Figure. 14 ORP result for Tx half-angle variations

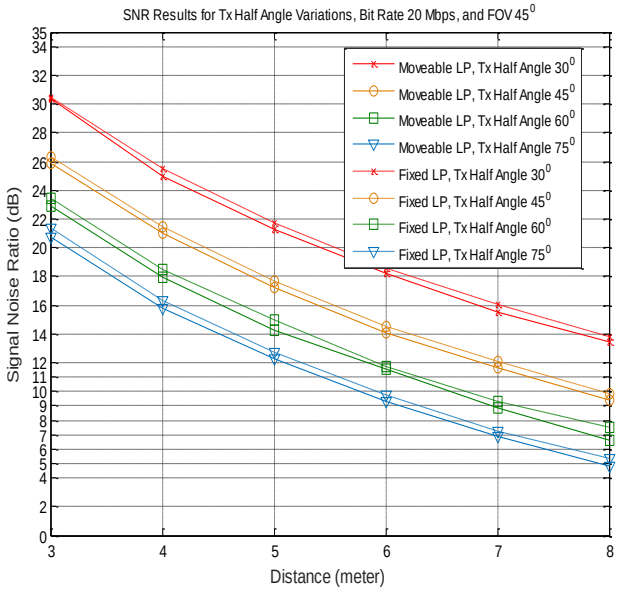

Figure. 15 SNR for Tx half-angle variations

increase the value of the transmitter half-angle. In that case, both parameters will decrease, where the value of 30° has the highest receiving power and SNR, as depicted in Fig. 14 and 15. The narrow transmitter angle proves that the reception power will be more focused, so the quality of the received signal will increase, but it impacts the acceptance area. The average power drop is 3 dBm with a decrease in SNR of 4 dB to 5 dB per meter.

4.3 FOV variation

The next test varies the FOV limited to using a bit rate of 20 Mbps and a half-angle transmitter value of 60° ($m = 1$). This reception angle affects the effective reception area related to the detector area, filter transmission gain, lens gain, and concentrator refractive index, as in Eqs. (9) to (11). Therefore, a high FOV value corresponds to a wide photodetector reception area. The FOV variations set in this experiment are 45°, 60°, and 90°. The amount of power received and SNR on the receiver side will be affected. The test results show significant differences related to the shape of the received spectrum due to differences in FOV values at a distance of 3 m, as depicted in Fig. 16 to 18.

The test results show significant differences in the shape of the spectrum received due to differences in FOV values, as depicted in Fig. 16 to 18. Almost the entire spectrum of the FOV

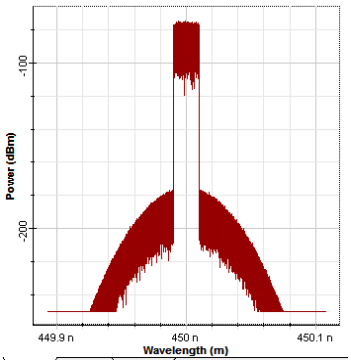

Figure. 16 Optical received spectrum for FOV of 45°

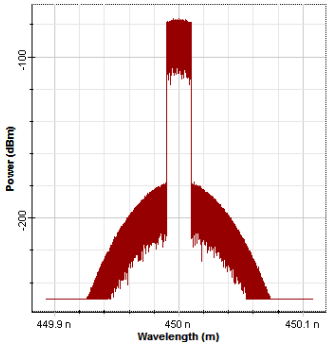

Figure. 17 Optical received spectrum for FOV of 60°

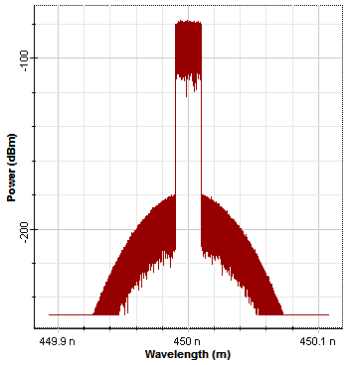

Figure. 18 Optical received spectrum for FOV of 90°

45° signal has an amplitude above −100 dBm. Therefore, large FOV values, such as 60° and 90°, correspond to a great signal spectrum that will cross the −100 dBm limit. This value will affect the reception power of the photodetector and the current detection results.

The received power and SNR values decreased drastically, approaching the limit of responsiveness for both fixed and movable LP schemes at a distance of 6 m to 8 m for all FOV variations, as shown in Fig. 19 and 20. Only FOV 45° has a higher reception power of −35 dBm and SNR of more than 6 dB at a distance of 8 m. The receiving power is in the range of −35 dBm to −37 dBm. The SNR value is less than 6 dB for the FOV values of 60° and 90° at a distance of 7 and 8 m. Low reception power and SNR will reduce the quality of the received signal.

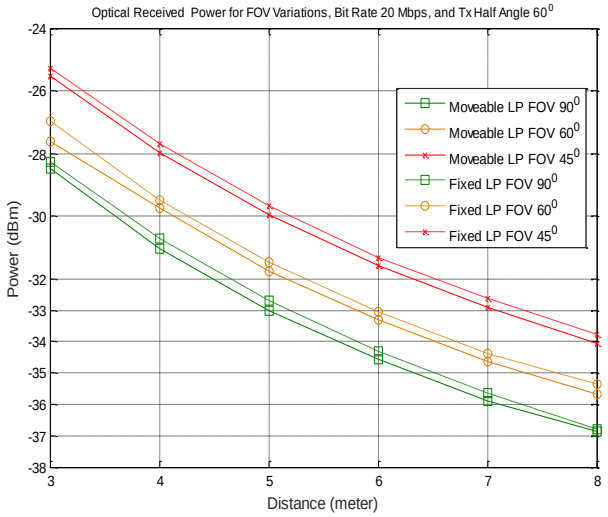

Figure. 19 ORP result for FOV variations

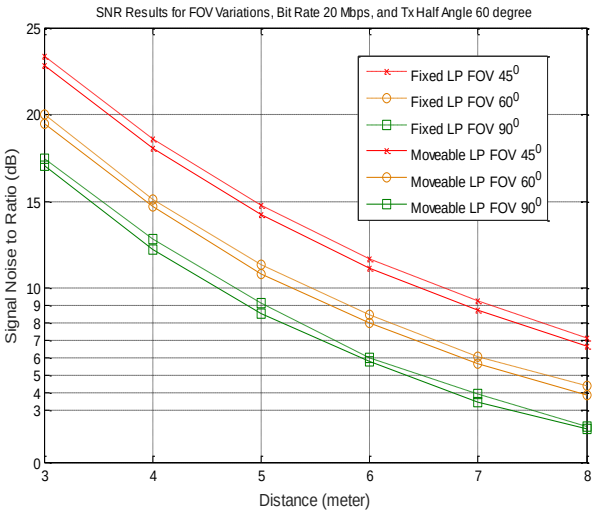

Figure. 20 SNR for FOV variations

Fig. 21 and 22 show that the increase in the slope in the BER value and the decrease in the Q factor are sharp. At a distance of 3 m, all FOV variations have a BER value below 10^{-60}. As the distance increases, the BER value becomes larger, where at a distance of 6 m, only FOV 45° has a value below 10^{-30} and even increases to 10^{-16} at a distance of 8 m. The problem lies in the distance of 7 m to 8 m, where BER is greater than 10^{-12} for FOV 60° and FOV 90°. Likewise, the Q factor for all variations of FOV is more than 17 at a 3 m distance, but it decreases as the distance increases. In contrast, at a distance of 6 m, the FOV 45° scenario had a Q factor of 13 and decreased to 8 at a distance of 8 m. The problem lies in the distance value of 7 m to 8 m, where BER is greater than 10^{-12} for FOV 60° and FOV 90°.

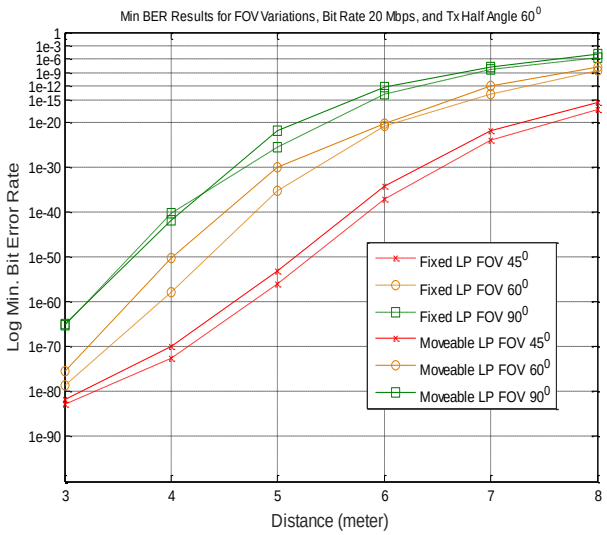

Figure. 21 Min BER result for FOV variations

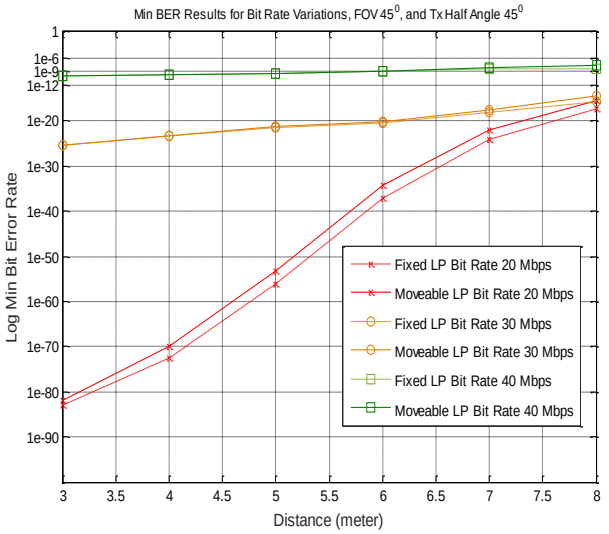

Figure. 23 Min BER result for bit rate variations

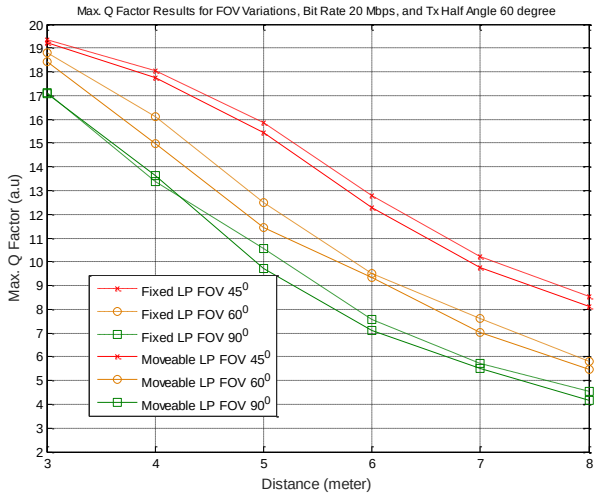

Figure. 22 Max Q-factor result for FOV variations

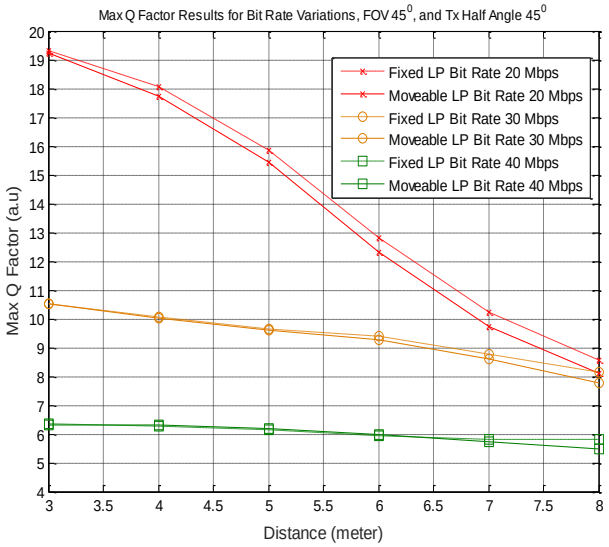

Figure. 24 Max Q-factor for bit rate variations

4.4 Bit rate variation

The researchers applied bit rate variations to determine the suitability of channel coding, frequency, bandwidth, and direct modulation mechanism on the transmitter side and the response and signal processing system on the receiver side. The tests use transmitter half-angle 45° and FOV 45° values using 20, 30, and 40 Mbps bit rates. Fig. 23 and 24 show that an increase in the bit rate results in a significant increase in the BER value and a decrease in the Q factor. For example, the 30 Mbps bit rate scenario has a BER value of 10^{-26} for the fixed and movable LED panel schemes at a distance of 3 m. Although adding the distance does not significantly change the BER value slope, at a distance of 8 m, the BER value is already in the range of 10^{-15}. This result differs from the 40 Mbps bit rate, where the BER value is 10^{-9} starting from 4 m to 8 m.

For the Q factor, the 30 Mbps bit rate scenario has a Q factor of 10.5 for the fixed and movable LED panel schemes at a distance of 3 m. Therefore, the obtained performance is fairly good for up to a distance of 6 m. After that, the added distance causes the value to decrease until the Q factor becomes 7.6 at a distance of 8 m. As for the 40 Mbps bit rate variation, the Q factor is 6, starting from a distance of 4 m to 8 m. Therefore, the proposed indoor Li-Fi system scheme is reliable for a data rate of 30 Mbps. On the basis of the test results up to the 8 m transmission distance variation, the performance of the model with all wavelength variations meets the ITU-T standard. In contrast, the 40 Mbps speed variation, 75° half-angle transmitter variation, and 60° and 90° FOV variations do not meet the ITU-T standard.

5. Conclusion

The test results indicate that all wavelength variations meet the ITU-T standard up to a variation of the transmission distance of 8 m, where the use of fixed and movable LEDs does not significantly differ in performance. The wavelength parameter affects the signal quality due to the spectral response and emission of LEDs, where the wavelength of 450 nm has better performance for short distances. However, for distances up to 8 m, the wavelength of 650 nm performs better than other variations. Increasing the transmitter half-angle increased the BER value and decreased the Q factor drastically. A smaller FOV is more recommended, where the increase in distance results in a significant decrease in performance. The proposed system model can also be used for bit rates up to 30 Mbps, although it is reliable up to 6 m only. The two system models do not have a significant difference in performance. Thus, using movable LED instead of fixed LED will make the system more dynamic with a well-maintained LOS.

Acknowledgments

This work is supported by Photonic Laboratory of Institut Teknologi Telkom Purwokerto, Smart System Laboratory of Universitas Gadjah Mada, and Telecommunication Laboratory of Universitas Brawijaya. The authors would like to thank the Network Communication Research Group and LPPM of IT Telkom Purwokerto for supporting this research.

References

[1] F. Aftab, M. N. U. Khan, and S. Ali, "Light fidelity (Li-Fi) based indoor communication system", *Int. J. Comput. Netw. Commun.*, Vol. 8, No. 3, pp. 21-31, 2016.

[2] T. C. Bui, S. Kiravittaya, K. Sripimanwat, and N. H. Nguyen, "A comprehensive lighting configuration for efficient indoor visible light communication networks", *Int. J. Opt.*, Vol. 2016, 1-9, 2016.

[3] F. Aftab, "Potentials and challenges of light fidelity based indoor communication system", *Int. J. New Comput. Archit. their Appl.*, Vol. 6, No. 3, pp. 91-102, 2016.

[4] L. M. Matheus, A. B. Vieira, L. F. M. Vieira, M. A. M. Vieira, and O. Gnawali, "Visible light communication: concepts, applications and challenges", *IEEE Commun. Surv. Tutorials*, Vol. 21, No. 4, pp. 3204-3237, 2019.

[5] D. B. Kuttan, S. Kaur, B. Goyal, and A. Dogra, "Light Fidelity: A future of wireless communication", In: *Proc. of 2021 2nd Int. Conf. Smart Electron. Commun. ICOSEC*, pp. 308-312, 2021.

[6] V. Swetha and E. Annadevi, "Survey on light-fidelity", In: *Proc. of International Conference on Smart Systems and Inventive Technology (ICSSIT 2018)*, pp. 355-358, 2018.

[7] P. Kuppusamy, S. Muthuraj, and S. Gopinath, "Survey and challenges of Li-Fi with comparison of Wi-Fi", In: *Proc. of 2016 IEEE Int. Conf. Wirel. Commun. Signal Process. Networking, WiSPNET 2016*, pp. 896-899, 2016.

[8] M. S. Chandra, S. Saleem, S. L. Harish, R. Baskar, and P. C. Kishoreraja, "Survey on Li-Fi technology and its applications", *Int. J. Pharm. Technol.*, Vol. 8, No. 4, pp. 20116-20123, 2016.

[9] J. I. Janjua, T. A. Khan, M. S. Khan, and M. Nadeem, "Li-Fi communications in smart cities for truly connected vehicles", In: *Proc. of 2nd 2021 Int. Conf. Smart Cities, Autom. Intell. Comput. Syst. ICON-SONICS 2021*, No. October, pp. 1-6, 2021.

[10] M. F. Tota, "Light Fidelity (Li-Fi) Communication Applied to Telepresence Robotics", *IEEE*, Vol. 59, p. 978, 2020.

[11] T. A. Nugraha and Y. Ardiyanto, "Li-Fi Technology for Transmitting Data in Hospital Environments", In: *Proc. of 1st Int. Conf. Inf. Technol. Adv. Mech. Electr. Eng. ICITAMEE 2020*, Vol. 0, pp. 81-84, 2020.

[12] S. Razzaq, N. Mubeen, and F. Qamar, "Design and analysis of light fidelity network for indoor wireless connectivity", *IEEE Access*, Vol. 9, pp. 145699-145709, 2021.

[13] H. D. Huynh and K. S. Sandrasegaran, "Coverage performance of light fidelity (Li-Fi) network", In: *Proc. of 2019 25th Asia Pac. Conf. Commun. APCC 2019*, pp. 361-366, 2019.

[14] S. K. Yaklaf and K. S. Tarmissi, "Multi-carrier modulation techniques for light fidelity technology", In: *Proc. of 19th Int. Conf. Sci. Tech. Autom. Control Comput. Eng. STA 2019*, pp. 70-73, 2019.

[15] H. D. Huynh, K. Sandrasegaran, and S. C. Lam, "Modelling and simulation of handover in light fidelity (Li-Fi) network", In: *Proc. of IEEE Reg. 10 Annu. Int. Conf.*, Vol. October, pp. 1307-1312, 2019.

[16] H. Haas, "Visible light communication", In: *Proc. of Opt. Fiber Commun. Conf. of C 2015*, 2015.

[17] S. Juneja and S. Vashisth, "Indoor positioning system using visible light communication", In:

Proc. of 2017 Int. Conf. Comput. Commun. Technol. Smart Nation, IC3TSN 2017, Vol. 2017-Octob, No. 978, pp. 79-83, 2017.

[18] R. Riaz, S. S. Rizvi, F. Riaz, S. Shokat, and N. A. Mughal, "Designing of cell coverage in Light Fidelity", *Int. J. Adv. Comput. Sci. Appl.*, Vol. 9, No. 3, pp. 44-53, 2018.

[19] R. G. N. Sendani, "Study the effect of FOV in visible light communication", *Int. Res. J. Eng. Technol.*, Vol. 4, No. 10, pp. 759-763, 2017.

[20] C. Chen, I. Tavakkolnia, M. D. Soltani, M. Safari, and H. Haas, "Hybrid multiplexing in OFDM-based VLC systems", In: *Proc. of 2020 IEEE Wirel. Commun. Netw. Conf. WCNC*, pp. 1-6, 2020.

[21] V. V. Andreev, "Wireless technologies of information transmission based on the using of modulated optical radiation (Li-Fi communication system): State and prospects", In: *Proc. of 2018 Syst. Signal Synchronization, Gener. Process. Telecommun. SYNCHROINFO*, Vol. 2018, pp. 1-4, 2018.